

Electronic supplementary information (ESI):

Aromatic sulfonium polyoxomolybdates: tuning the photochromic properties through substitutions on the counter ion moiety

Ashwani Kumar,^a Chullikkattil P. Pradeep*^a

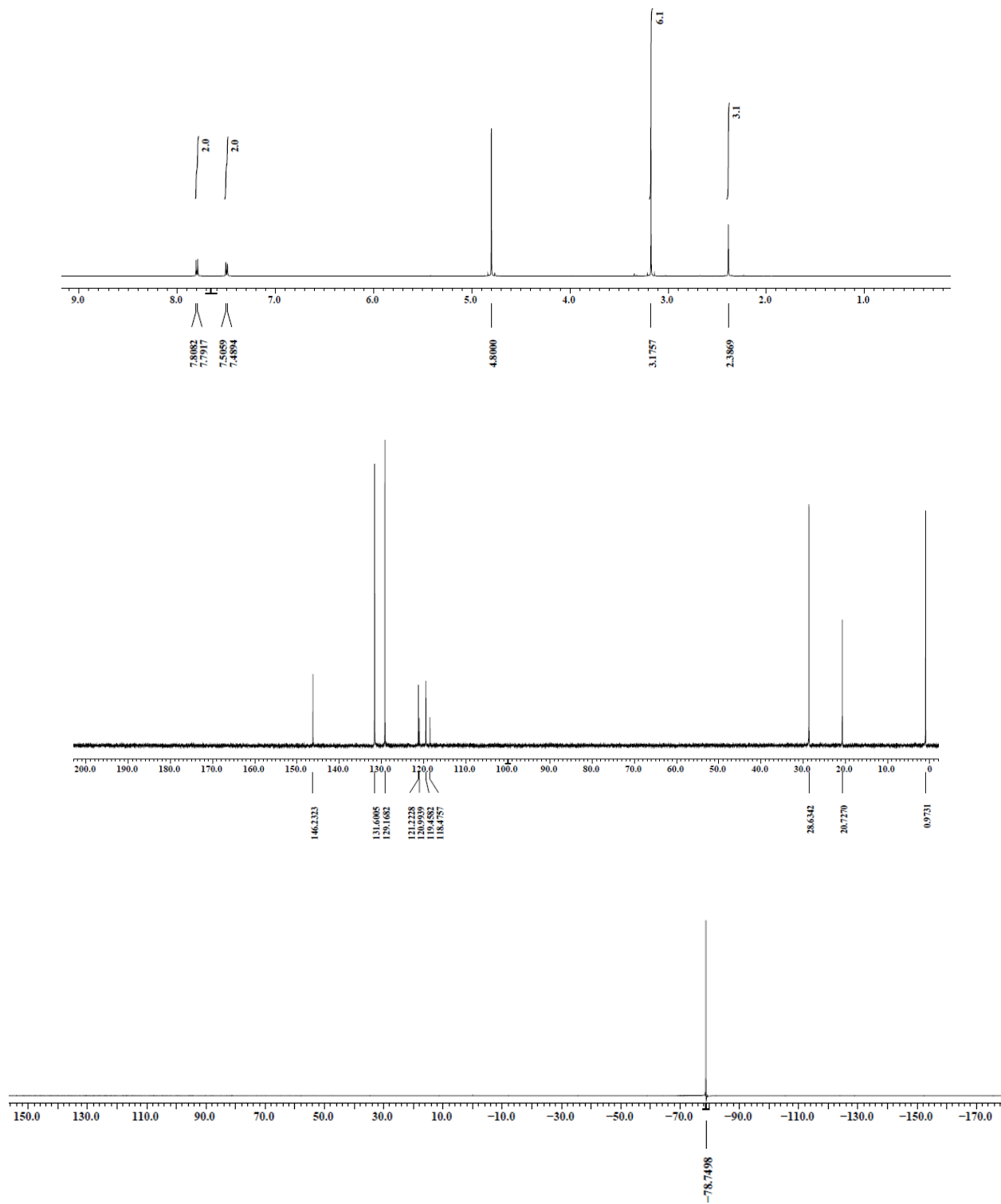


Figure S1. ¹H, ¹³C and ¹⁹F NMR spectra of DMTST in D₂O.

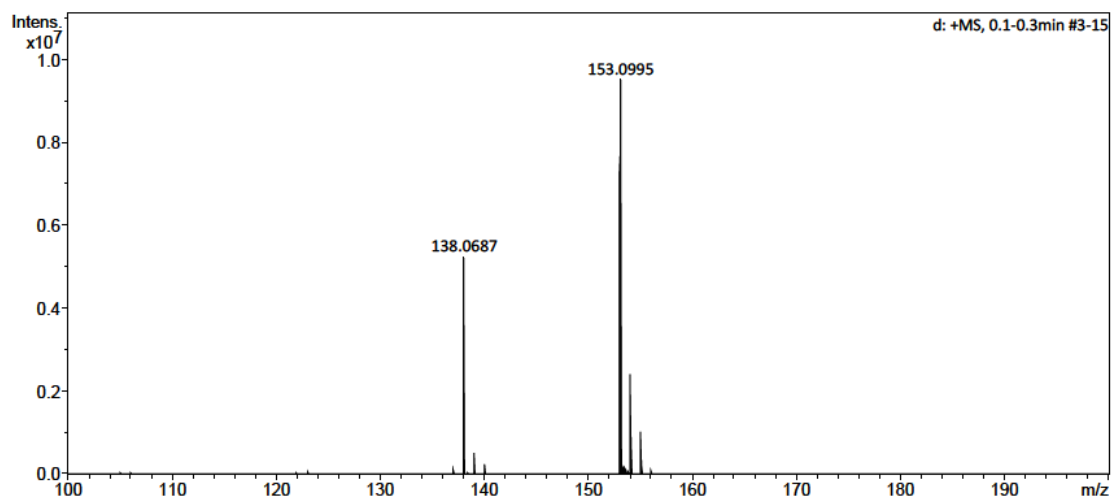


Figure S2. HR-MS of DMTST.

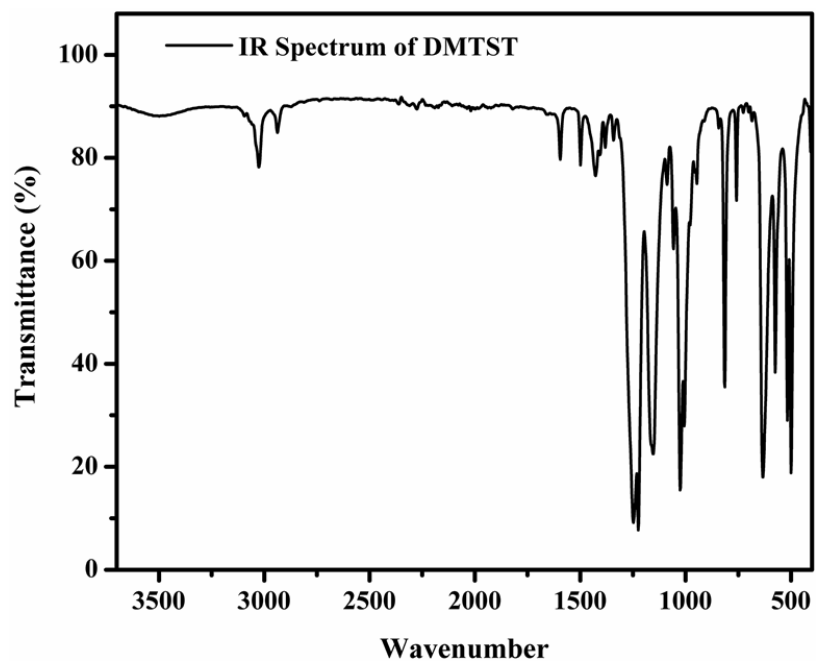


Figure S3. IR spectrum of DMTST.

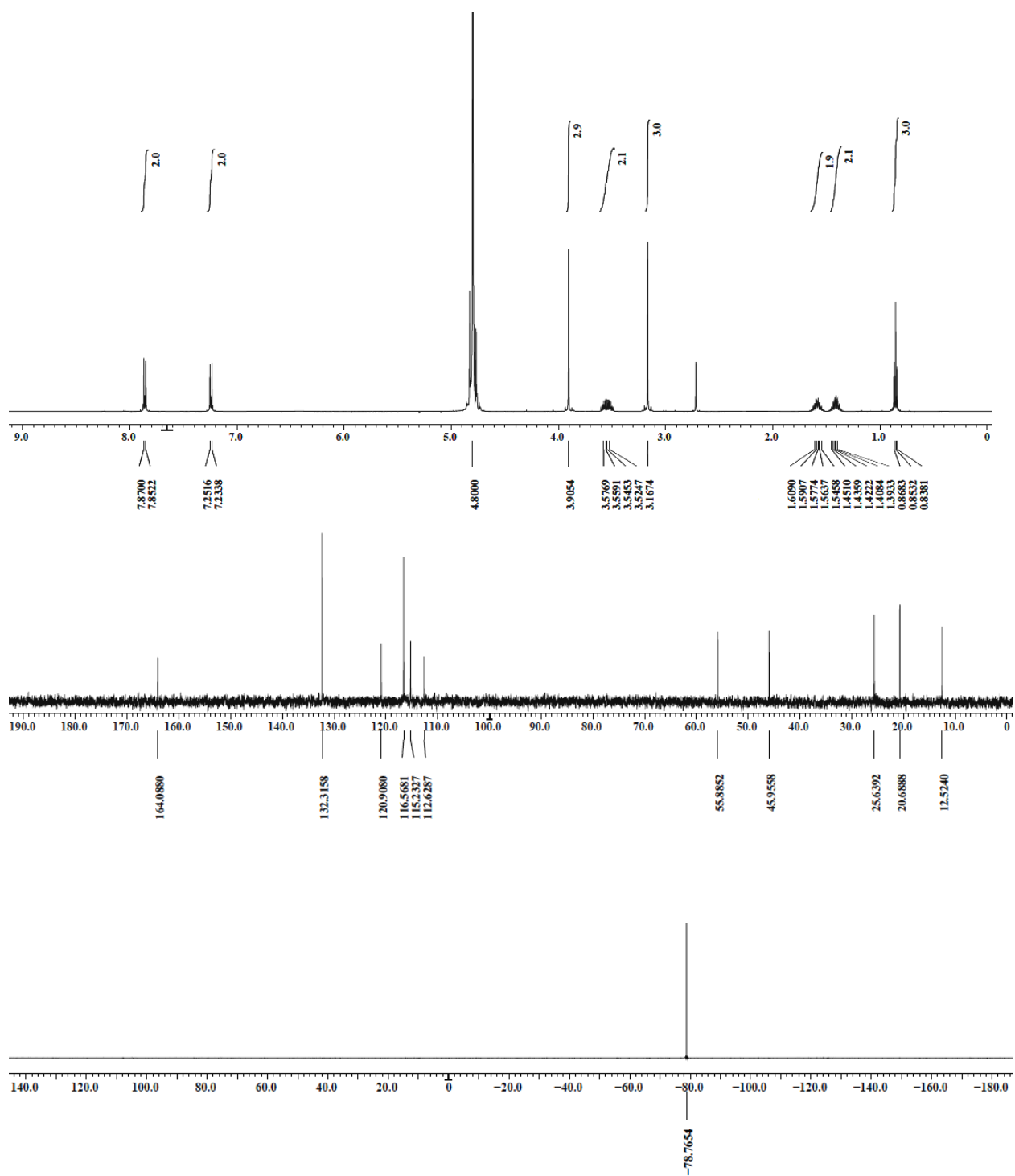


Figure S4. ¹H, ¹³C and ¹⁹F NMR spectra of BMPMST in D₂O.

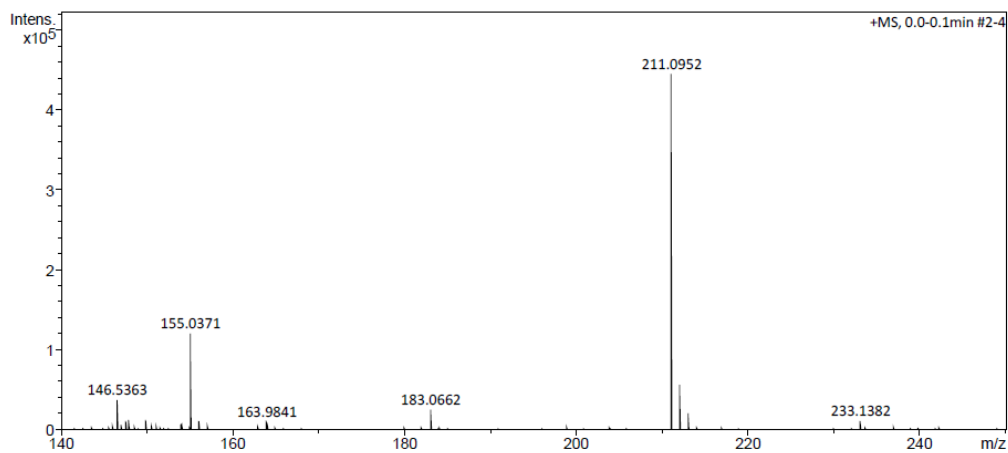


Figure S5. HR-MS of BMPMST.

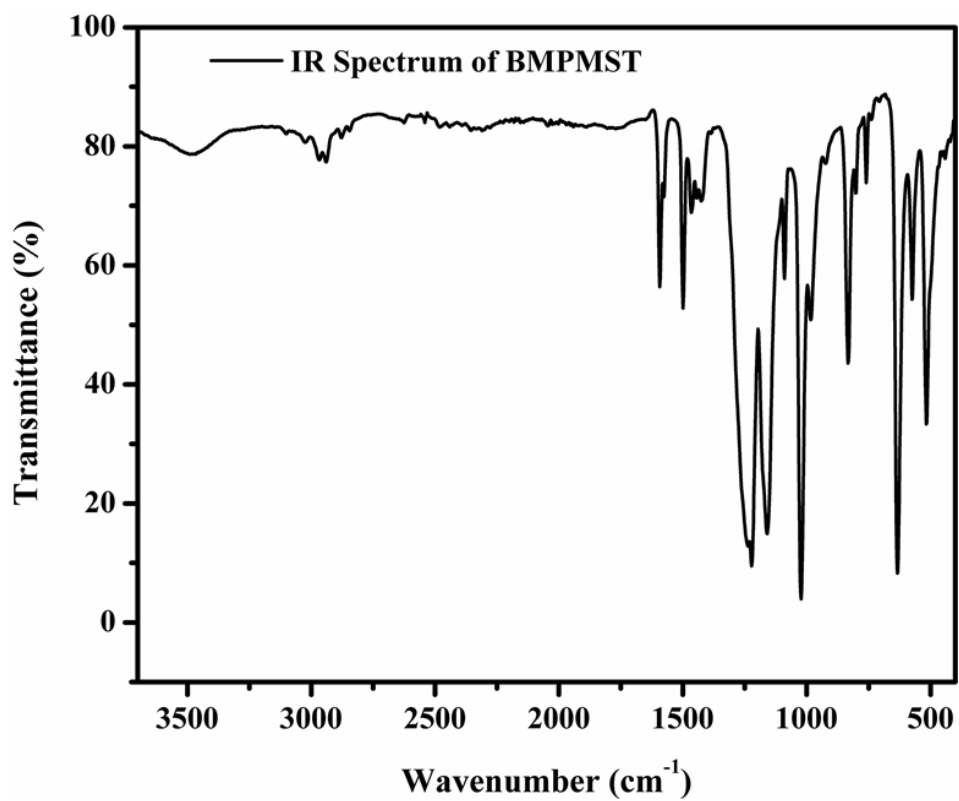


Figure S6. IR spectrum of BMPMST.

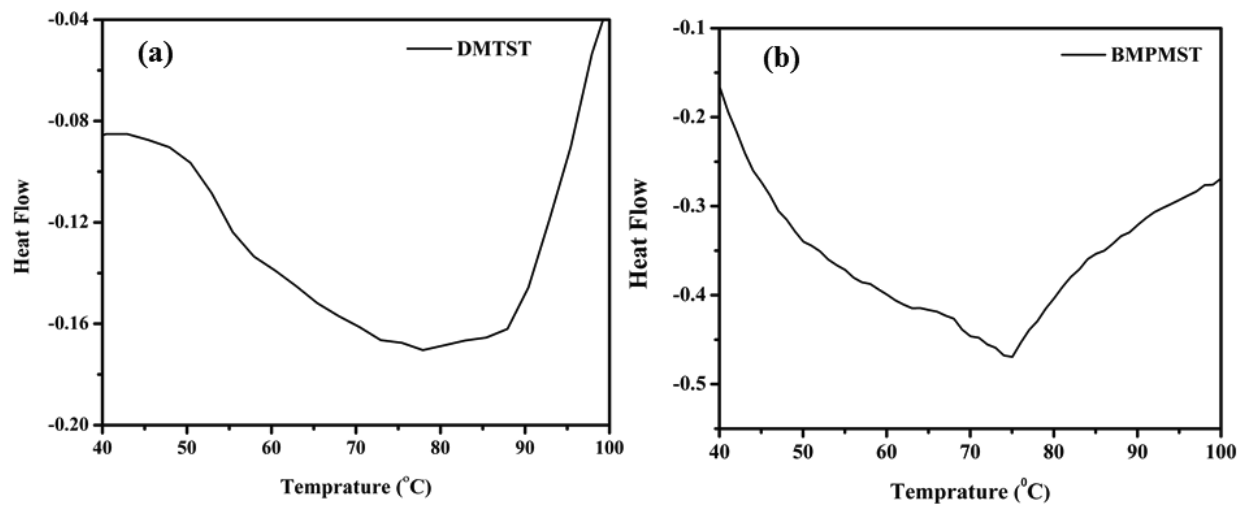


Figure S7. DSC curves of (a) DMTST and (b) BMPMST.

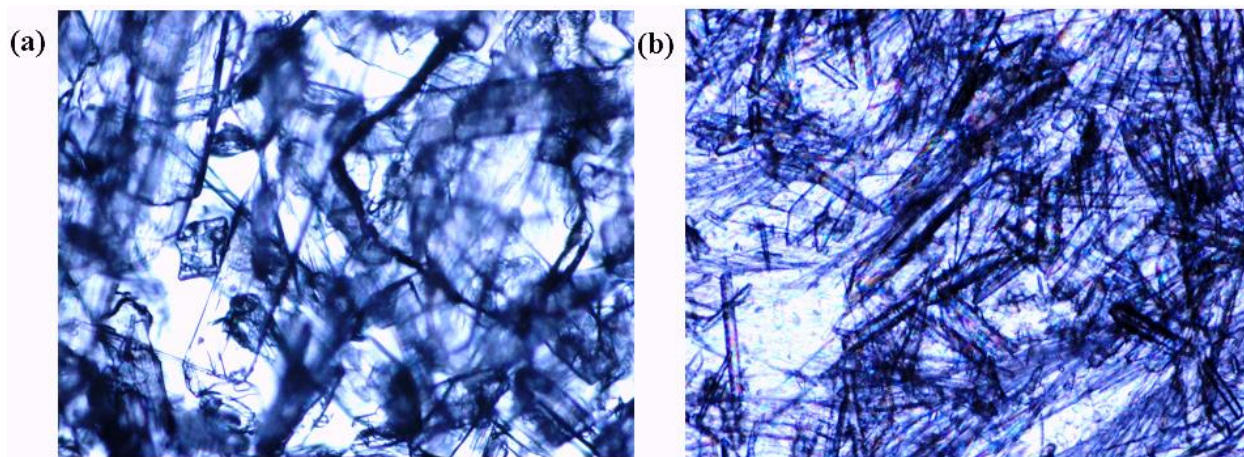


Figure S8. Polarised optical microscopic images of (a) DMTST and (b) BMPMST under crossed polariser at room temperature.

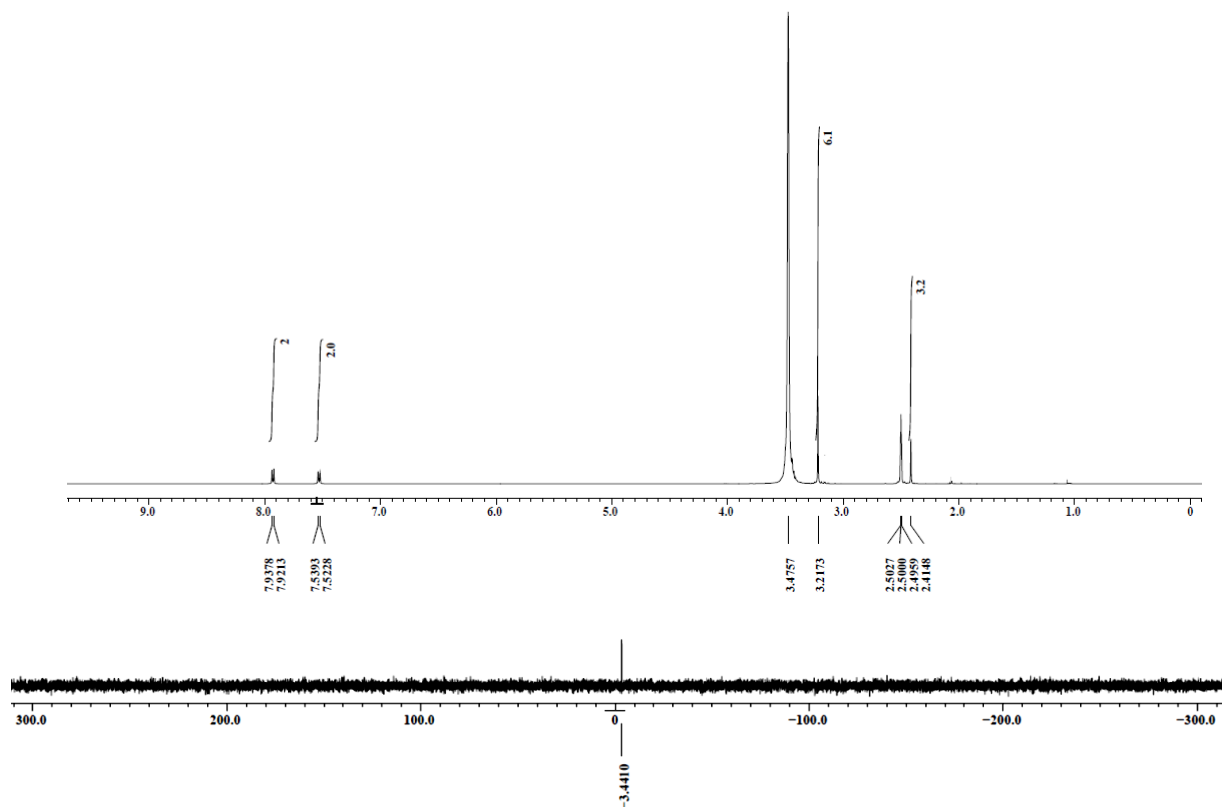


Figure S9. ¹H and ³¹P NMR spectra of hybrid 1 in DMSO-*d*₆.

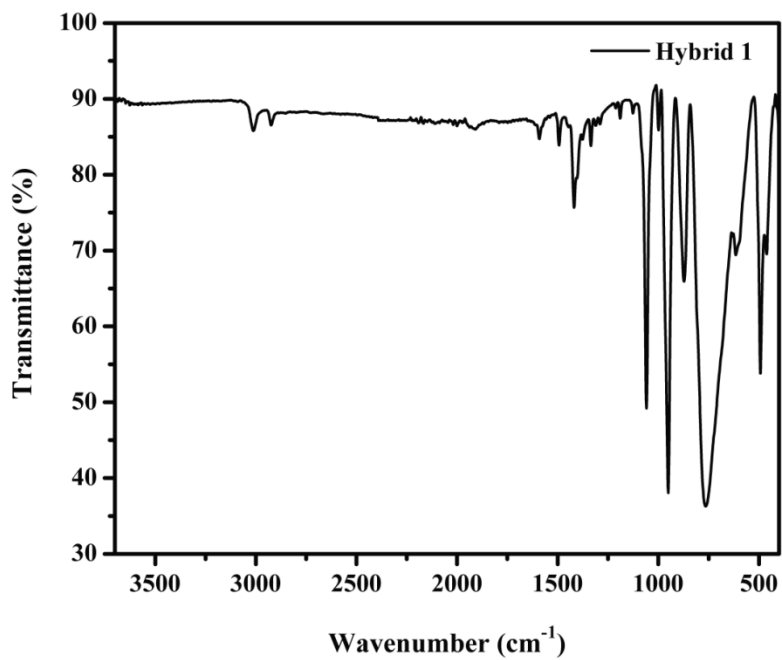


Figure S10. IR spectrum of hybrid 1.

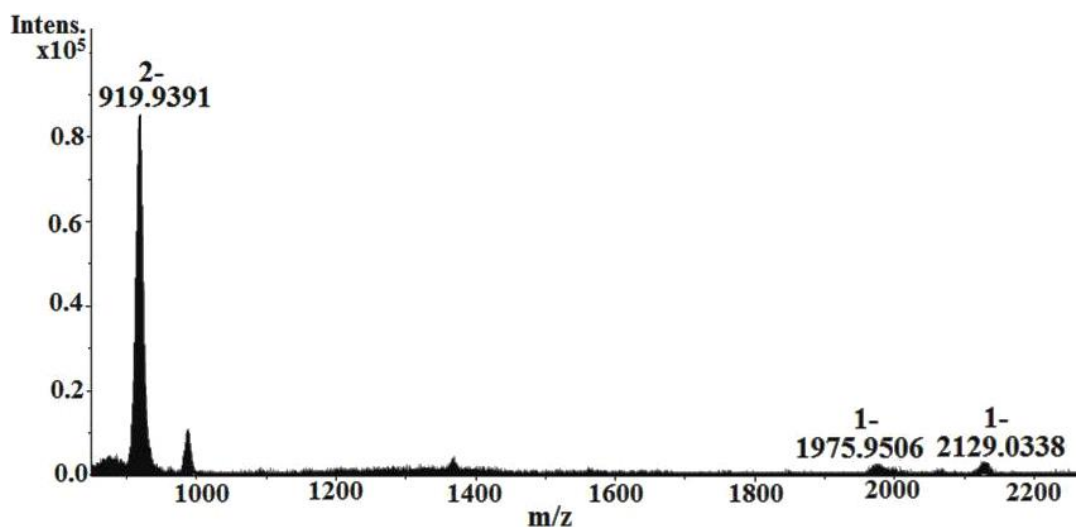


Figure S11. The negative ion mode ESI-MS of hybrid **1** in MeCN.

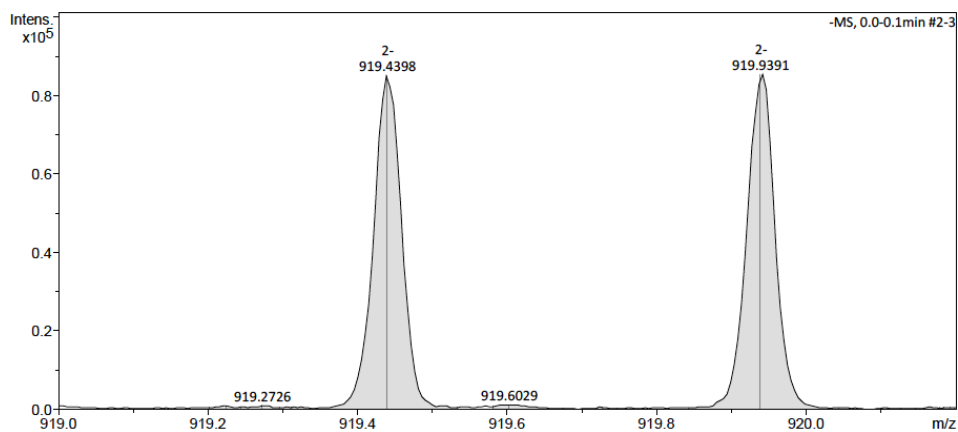


Figure S12. Zoom-in of the peak centered at m/z 919.9391 in the ESI-MS of hybrid **1** to show its 2^- charge state.

Table S1. Detailed assignment of mass spectral data for hybrid **1**.

No.	Ion (hybrid 1)	Charge	m/z calculated	m/z observed
1	$\text{H}[\text{PMo}_{12}\text{O}_{40}]^{2-} \cdot \text{H}_2\text{O}$	2^-	920.62	919.93
2	$\text{H}(\text{DMTS})[\text{PMo}_{12}\text{O}_{40}]^{1-}$	1^-	1976.34	1975.95
3	$(\text{DMTS})_2[\text{PMo}_{12}\text{O}_{40}]^{1-}$	1^-	2129.43	2129.03

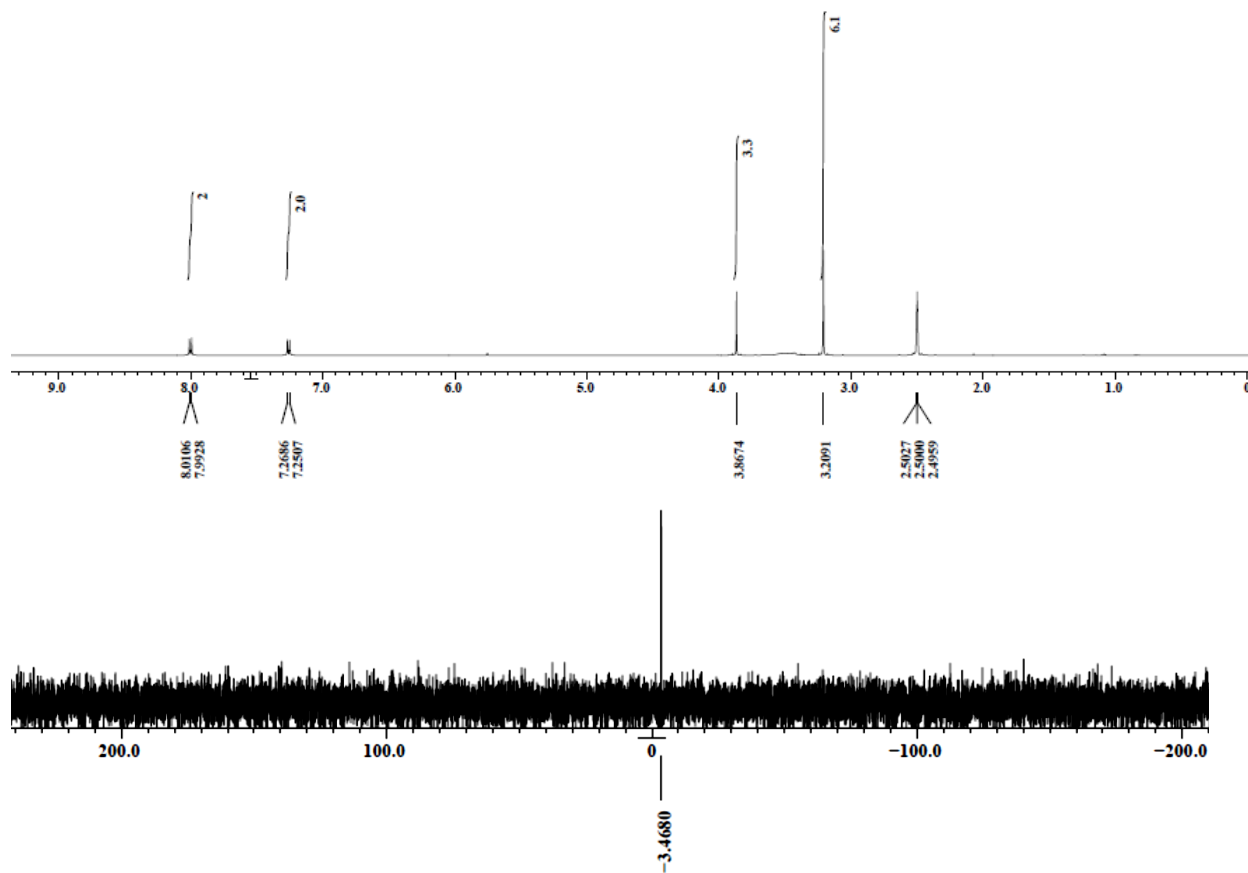


Figure S13. ¹H and ³¹P NMR spectra of hybrid 2 in DMSO-d₆.

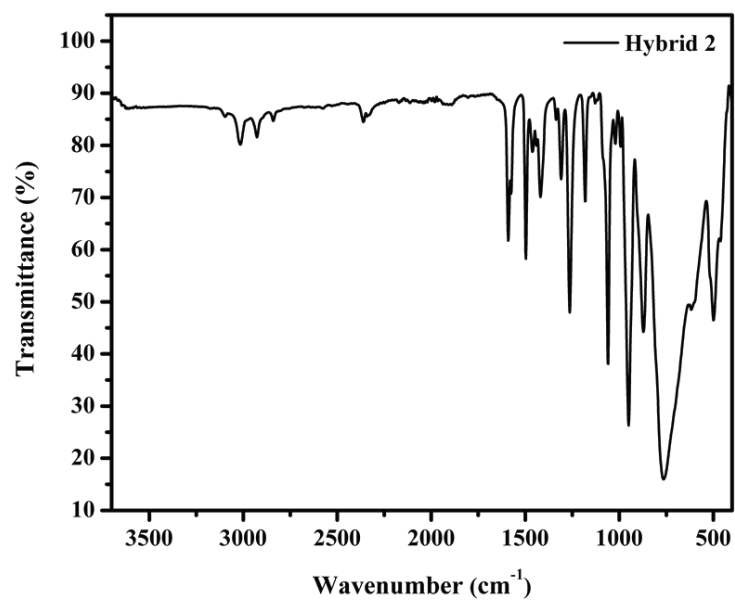


Figure S14. IR spectrum of hybrid 2.

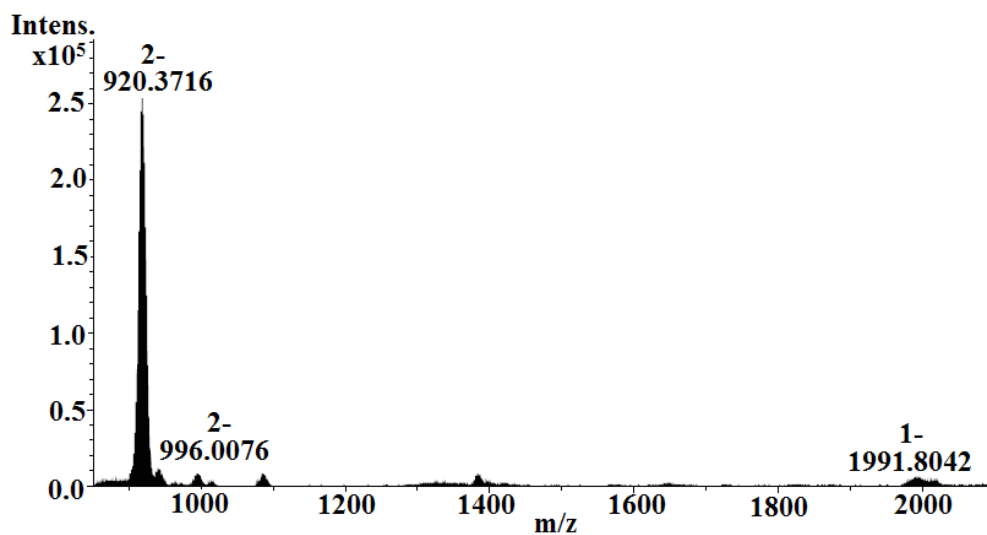


Figure S15. The negative ion mode ESI-MS of hybrid **2** in MeCN.

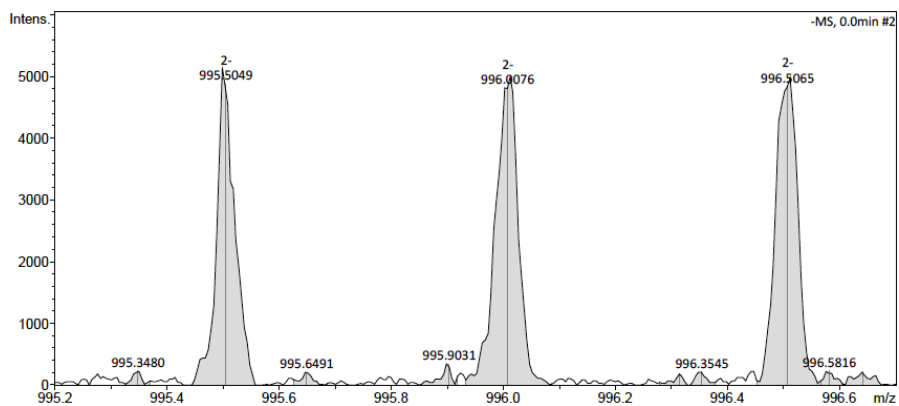


Figure S16. Zoom-in of the peak centered at m/z 996.0076 in the ESI-MS of hybrid **2** to show its 2^- charge state.

Table S2. Detailed assignment of mass spectral data for hybrid **2**.

No.	Ion (hybrid 2)	Charge	m/z calculated	m/z observed
1	$\text{H}[\text{PMO}_{12}\text{O}_{40}]^{2-} \cdot \text{H}_2\text{O}$	2^-	920.62	920.37
2	$(\text{MPDS})[\text{PMO}_{12}\text{O}_{40}]^{2-}$	2^-	995.65	996.00
3	$\text{H}(\text{MPDS})[\text{PMO}_{12}\text{O}_{40}]^{1-}$	1^-	1992.31	1991.80

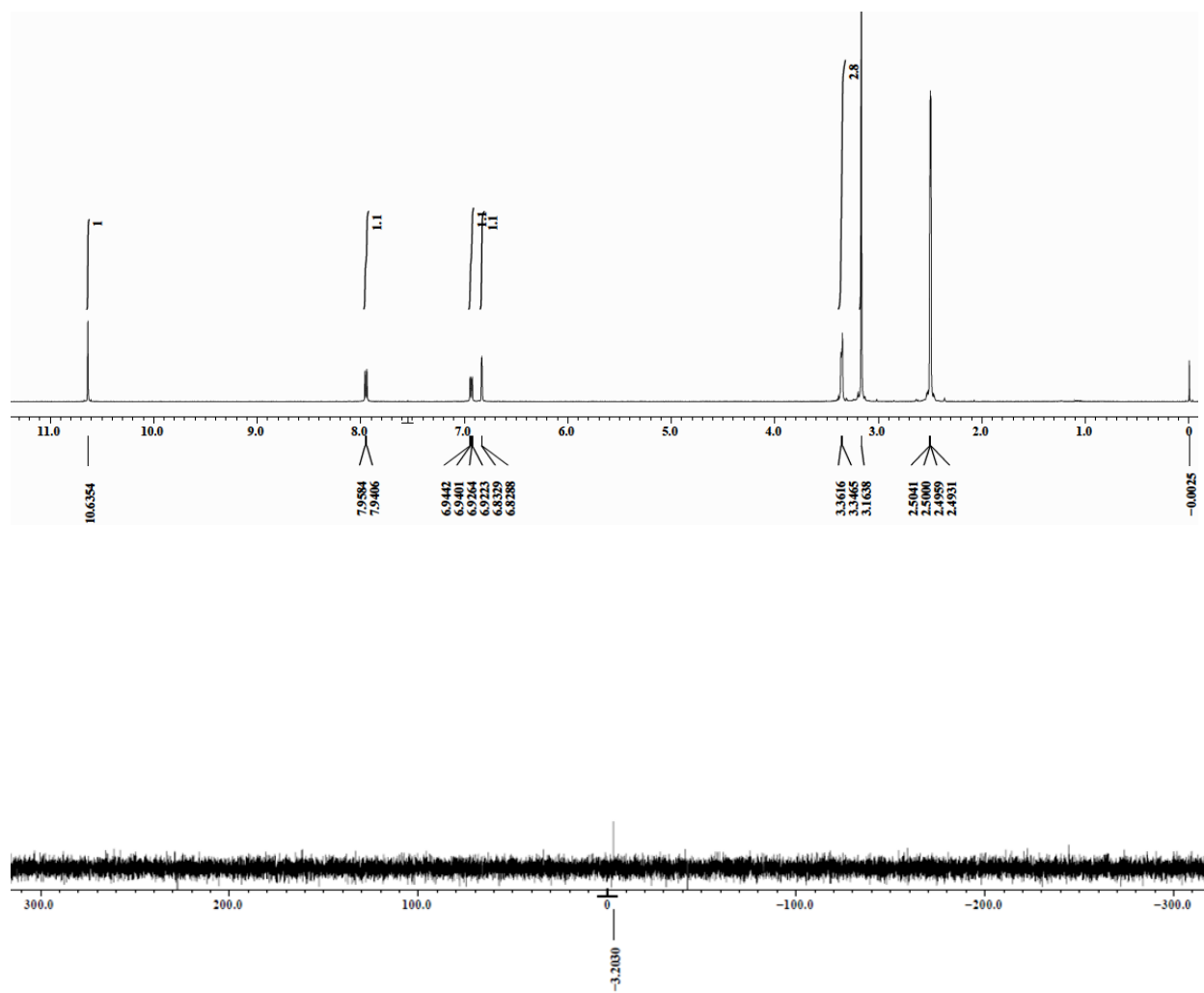


Figure S17. ¹H and ³¹P NMR spectra of hybrid 3 in DMSO-*d*₆.

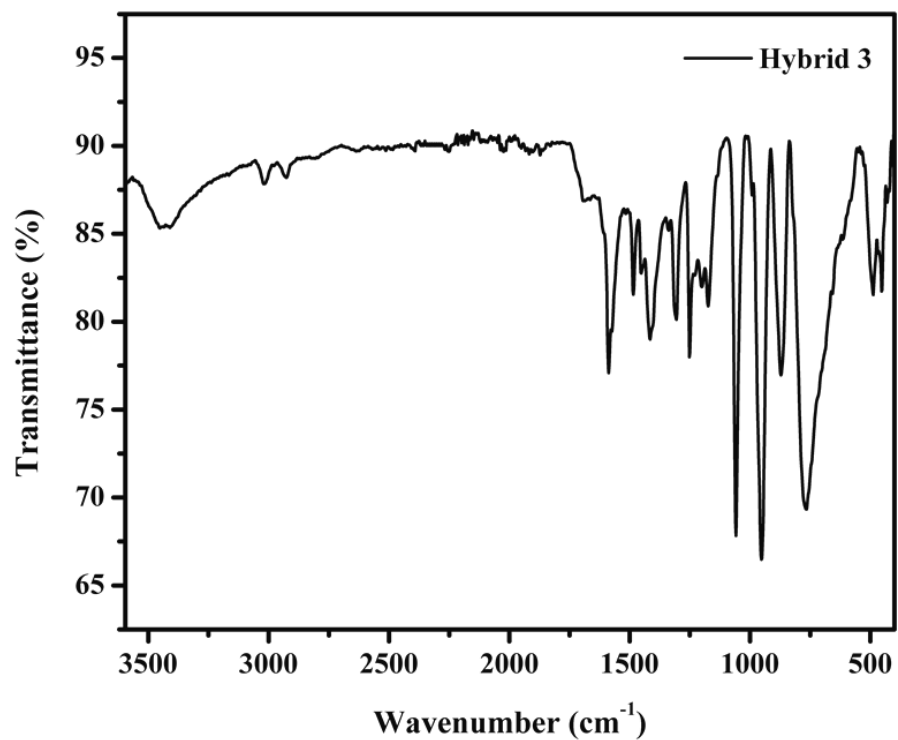


Figure S18. IR spectrum of hybrid **3**.

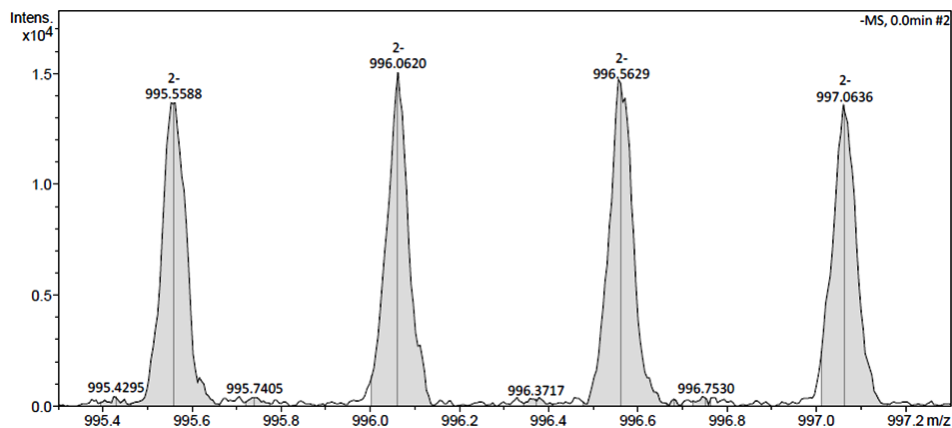


Figure S19. Zoom-in of the peak centered at m/z 996.0620 in the ESI-MS of hybrid **3** to show its 2^- charge state.

Table S3. Detailed assignment of mass spectral data for hybrid **3**.

No.	Ion (hybrid 3)	Charge	m/z calculated	m/z observed
1	$\text{H}[\text{PMo}_{12}\text{O}_{40}]^{2-}$	2-	911.62	911.01
2	$(\text{HMPDS})[\text{PMo}_{12}\text{O}_{40}]^{2-}$	2-	995.65	996.06
3	$\text{H}(\text{HMPDS})[\text{PMo}_{12}\text{O}_{40}]^{1-}$	1-	1992.31	1992.14
4	$(\text{HMPDS})_2[\text{PMo}_{12}\text{O}_{40}]^{1-}$	1-	2160.38	2160.25

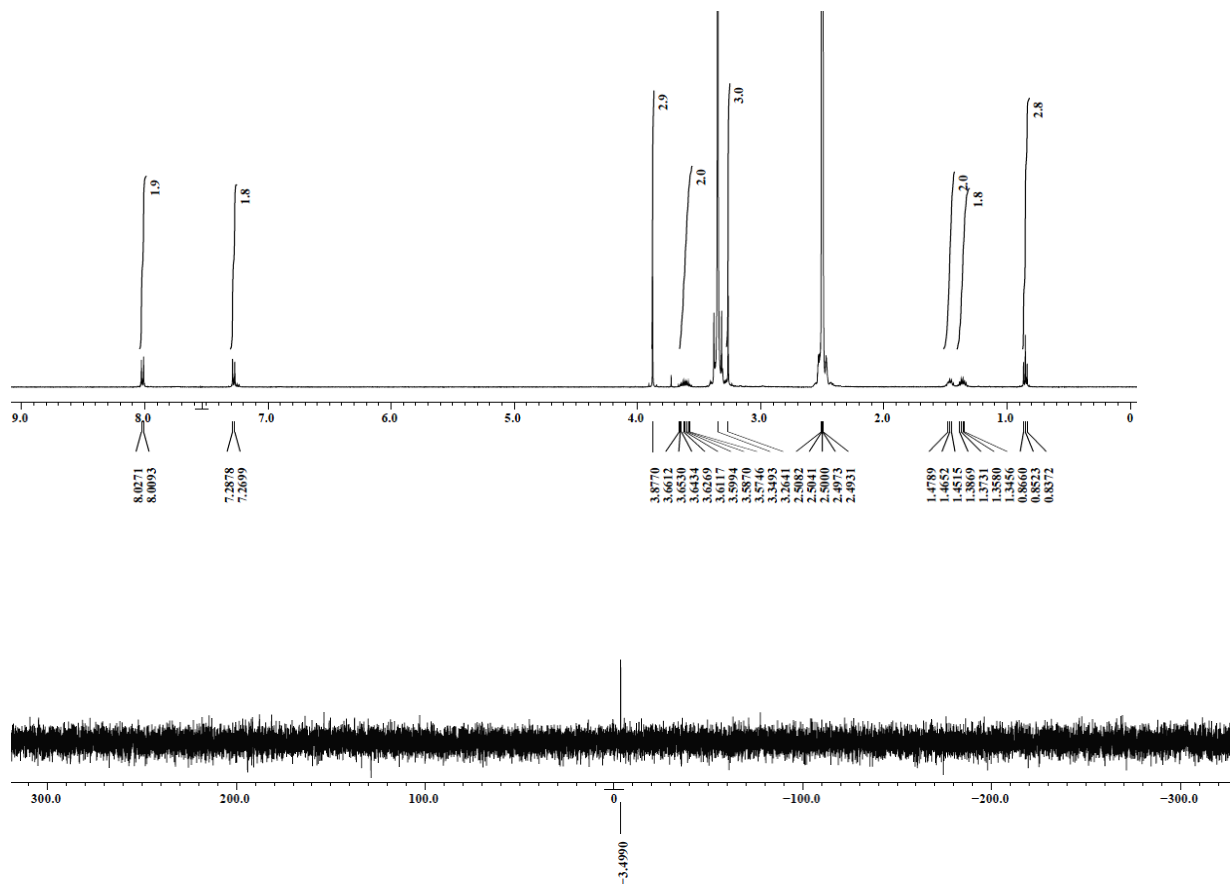


Figure S20. ¹H and ³¹P NMR spectra of hybrid **4** in DMSO-*d*₆.

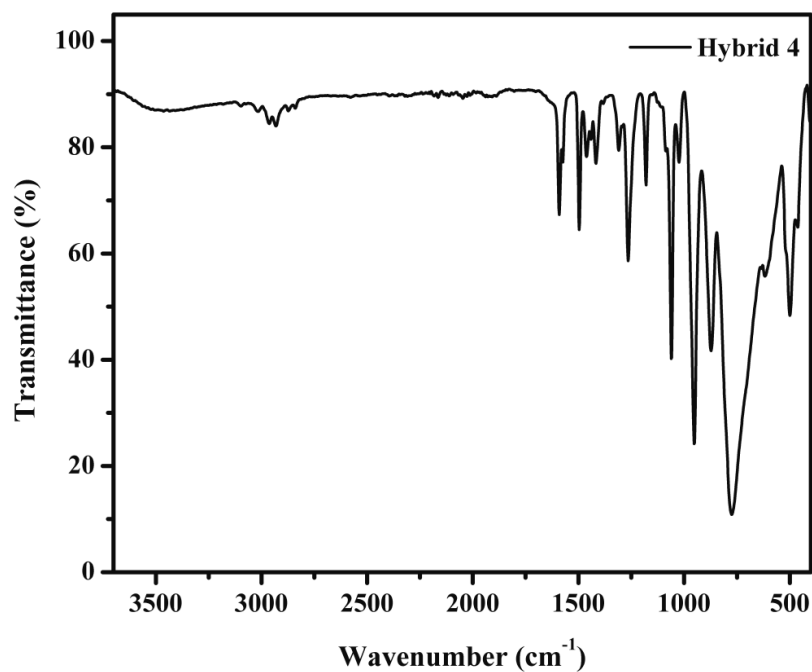


Figure S21. IR spectrum of hybrid 4.

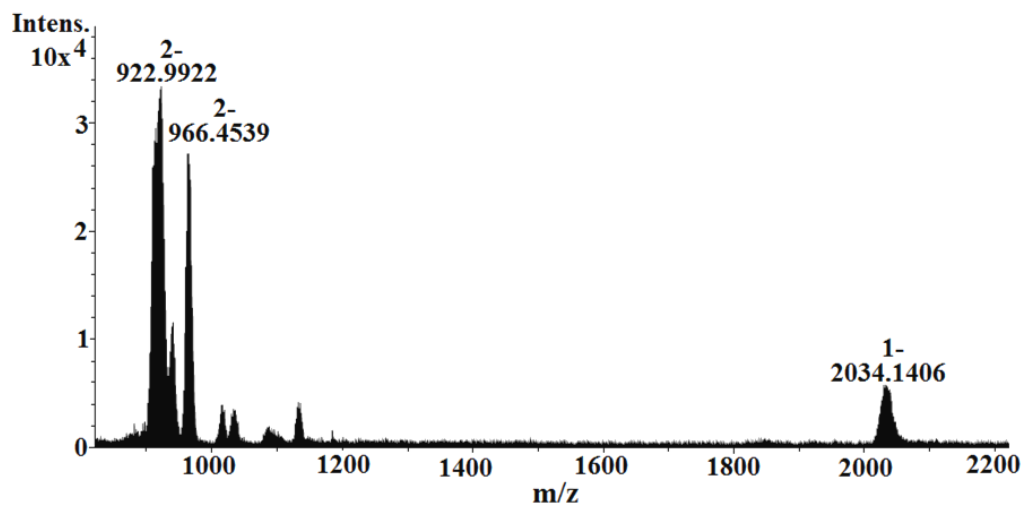


Figure S22. The negative ion mode ESI-MS of hybrid 4 in MeCN.

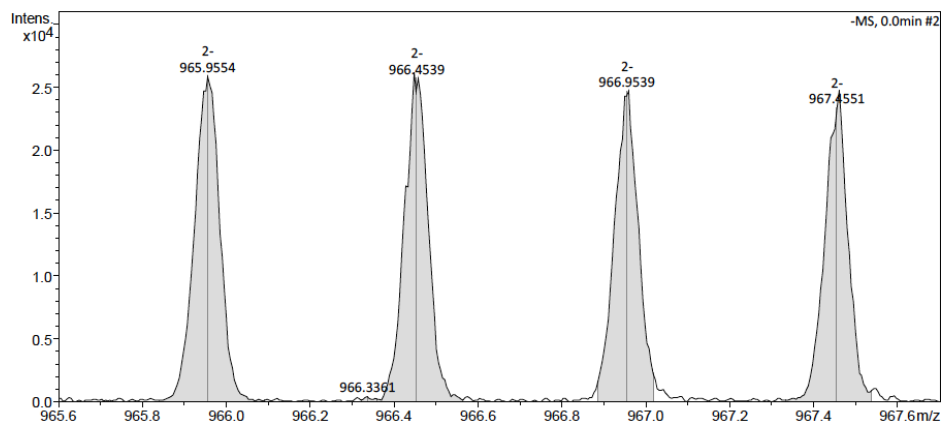


Figure S23. Zoom-in of the peak centered at m/z 966.4539 in the ESI-MS of hybrid **4** to show its 2^- charge state.

Table S4. Detailed assignment of mass spectral data for hybrid **4**.

No.	Ion (hybrid 4)	Charge	m/z calculated	m/z observed
1	$\text{Na}[\text{PMO}_{12}\text{O}_{40}]^{2-}$	2^-	922.62	922.99
2	$\text{K}[\text{PMO}_{12}\text{O}_{40}]^{2-} \cdot 4\text{H}_2\text{O}$	2^-	966.62	966.45
3	$\text{H}(\text{BMPMS})[\text{PMO}_{12}\text{O}_{40}]^{1-}$	1^-	2034.34	2034.14

Table S5. The crystallographic data and structure refinement parameters of hybrids **1**, **2** and **4**.

	Hybrid 1	Hybrid 2	Hybrid 4
Empirical formula	C ₂₇ H ₃₉ Mo ₁₂ O ₄₀ PS ₃	C ₂₇ H ₃₉ Mo ₁₂ O ₄₃ PS ₃	C ₃₆ H ₅₇ Mo ₁₂ O ₄₃ PS ₃
Formula weight	2282.01	2330.01	2456.25
T/K	293(2)	150.01(10)	149.99(10)
Wavelength/Å	0.71073	0.71073	1.54184
Crystal system	trigonal	trigonal	triclinic
Space group	R-3	R-3	P-1
<i>a</i> (Å)	20.3393(3)	20.1657(6)	12.4149(7)
<i>b</i> (Å)	20.3393(3)	20.1657(6)	12.6395(6)
<i>c</i> (Å)	23.9935(4)	24.1757(8)	23.2868(9)
α (°)	90.00	90.00	95.806(4)
β (°)	90.00	90.00	95.886(4)
γ (°)	120.00	120.00	115.353(5)
<i>V</i> (Å ³)	8596.0(3)	8514.0(4)	3241.7(3)
<i>Z</i>	6	6	2
D _c (Mg m ⁻³)	2.645	2.727	2.516
μ (mm ⁻¹)	2.767	2.800	20.380
<i>F</i> (000)	6528.0	6672.0	2368.0
Crystal size (mm ³)	0.342x0.167x0.068	0.271x0.136x0.114	0.165 × 0.127 × 0.072
2 θ (°)	4 to 56.76°	4.04 to 56.46°	7.74 to 133.96°
Reflections collected	5544	5396	21623
Independent reflections	4121[R(int) = 0.0170]	4083[R(int) = 0.0209]	11367[R(int) = 0.0443]
Data / restraints / parameters	4121/0/253	4083/0/262	11367/0/865
Goodness-of-fit on F ²	1.110	1.159	1.050
Final R indices [<i>I</i> > 2 σ (<i>I</i>)]	R1 = 0.0682, wR2 = 0.1424	R1 = 0.0860, wR2 = 0.1780	R1 = 0.0420, wR2 = 0.1072
R indices (all data)	R1 = 0.0741, wR2 = 0.1463	R1 = 0.0894, wR2 = 0.1797	R1 = 0.0500, wR2 = 0.1141
Largest diff. peak and hole (e.Å ⁻³)	3.59 and -1.42	4.82 and -2.37	4.07/-1.22

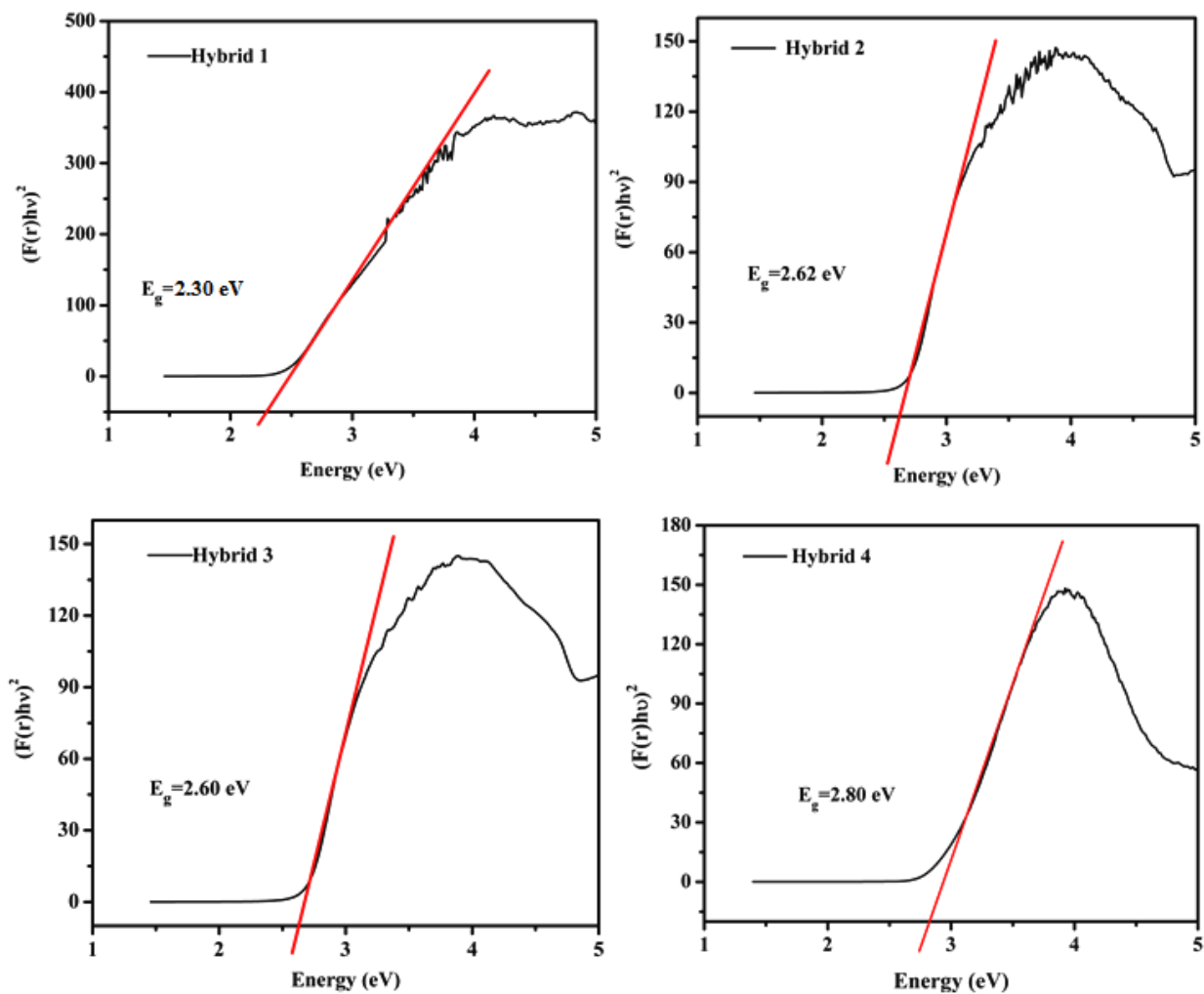


Figure S24. UV-Vis diffuse reflectance spectra: Kubelka-Munk (K-M) function vs energy (eV) plots of hybrids 1–4.

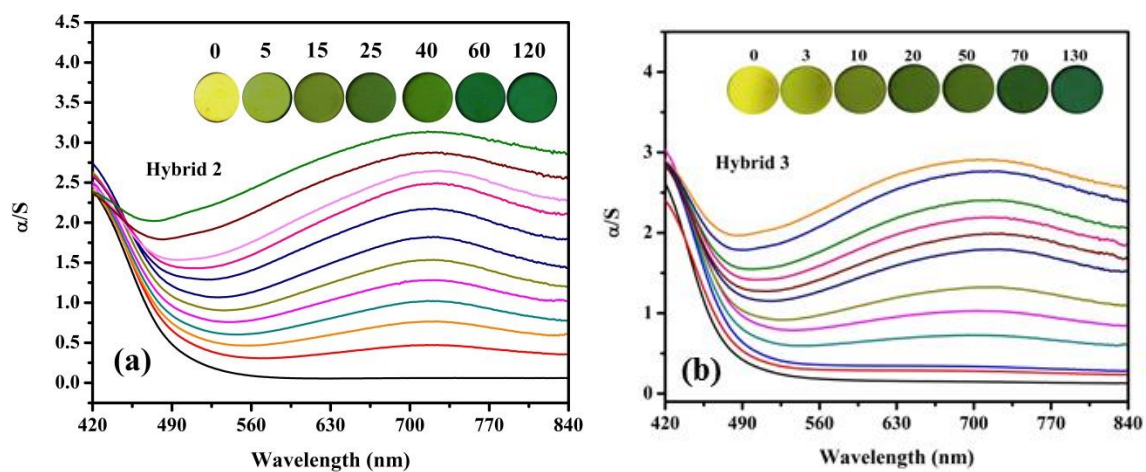


Figure S25. Kubelka-Munk (K-M) transformed reflectivity of (a) hybrid 2 and (b) hybrid 3 after irradiation with 350 nm UV lamp at various time intervals. Inset: the color change after various intervals of time.

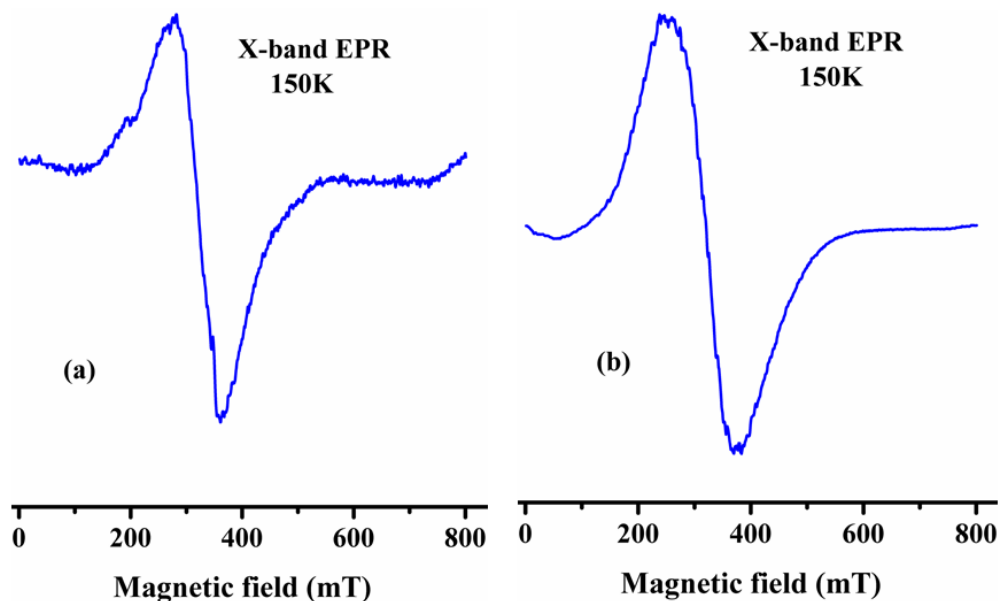


Figure S26. Powder X-band EPR spectra (recorded at 293 K) for (a) hybrid 3 and (b) hybrid 4 after irradiation with 350 nm UV lamp at 9.451, 9.452 GHz spectrometer frequencies respectively.

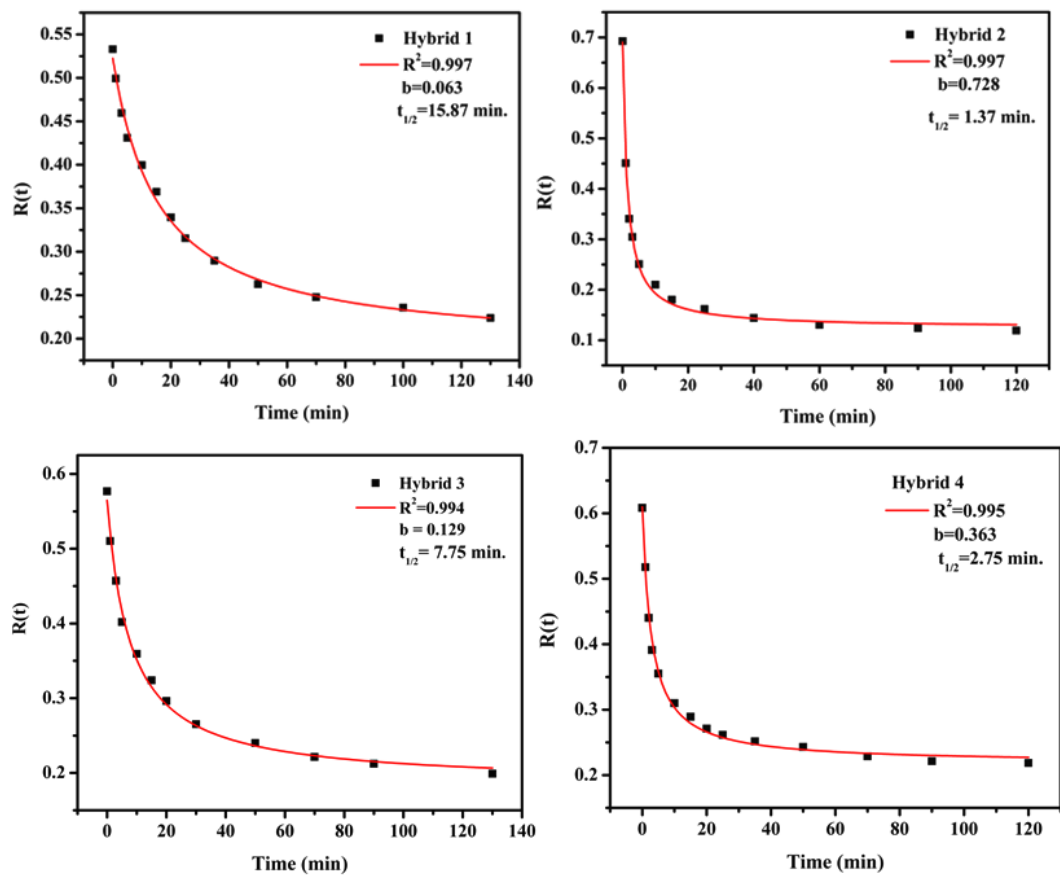


Figure S27. Reflectivity vs time plots for hybrids 1-4.

Table S6. Optical characteristics and coloration kinetics parameters of hybrids 1-4.

	Hybrid 1	Hybrid 2	Hybrid 3	Hybrid 4
$\lambda_{\max}(\text{nm})^p$	710	710	700	730
$R^{\lambda_{\max}}(0)^q$	0.533	0.693	0.576	0.608
R^{2r}	0.997	0.997	0.994	0.995
b^s	0.063	0.728	0.129	0.363
R^{2r}	0.998	0.999	0.999	0.999
B^t	0.347	0.956	0.540	0.699
$t_{1/2}^u$	15.87	1.37	7.75	2.75

^pPhoto-induced absorption band wavelength.

^qReflectance value before UV irradiation ($t = 0$) at λ_{\max} .

^rRegression coefficient.

^sSalient coloration kinetic parameter.

^tColoration kinetics parameters for the linear relation $[R_{\lambda_{\max}}(t) - R_{\lambda_{\max}}(\infty)]^{-1} = Bt + A$.

^uHalf life time (min.) of photochromic process.

Table S7. Comparison of the minimum coloration kinetics half-life times of some reported photochromic hybrid POMs.

Sr. No.	Hybrid POM	Minimum coloration kinetic half life time ($t_{1/2}$) obtained	Reference
1	(MPDS) ₃ [PMO ₁₂ O ₄₀] (Hybrid 2)	1.37 min	Present work
2	(MPDS) ₄ [Mo ₈ O ₂₆]	0.33 min	Ref. 1
3	NaKMo ₆ (Ale-4Py) ₂	0.37 min	Ref. 2
4	(H ₂ DABCO) ₂ (HDMA) _{0.5} Na _{0.75} (H ₃ O) _{0.75} [Mo ₈ O ₂₇]·3H ₂ O	0.8 min	Ref. 3
5	(APDS) ₄ [SiMo ₁₂ O ₄₀]	1.01 min	Ref. 4
6	(Mo ₆ -Ale)	2.87 min	Ref. 5
7	Rb _{0.75} (NH ₄) _{5.25} [(Mo ₃ O ₈) ₂ O(O ₃ PC(CH ₂ S(CH ₃) ₂)-OPO ₃) ₂]·8H ₂ O	4.84 min	Ref. 6
8	Na ₇ (N(C ₄ H ₉) ₄)[(Mo ₃ O ₈) ₄ (O ₃ PC(C ₃ H ₆ NH ₃)(O)PO ₃) ₄].43H ₂ O	7.40 min	Ref. 7

References

- 1 A. Kumar, A. K. Gupta; M. Devi, K. E. Gonsalves and C. P. Pradeep, *Inorg. Chem.*, 2017, **56**, 10325.
 - 2 O. Oms, T. Benali, J. Marrot, P. Mialane, M. Puget, H. Serier-Brault, P. Deniard, R. Dessapt and A. Dolbecq, *Inorganics*, 2015, **3**, 279.
 - 3 R. Dessapt, M. Collet, V. Coue, M. Bujoli-Doeuff, S. Jobic, C. Lee and M.-H. Whangbo, *Inorg. Chem.*, 2009, **48**, 574.
 - 4 A. Kumar, M. Devi, N. Mamidi, K. E. Gonsalves and C. P. Pradeep, *Chem. Eur. J.*, 2015, **21**, 18557.
 - 5 H. E. Moll, A. Dolbecq, I. M. Mbomekalle, J. Marrot, P. Deniard, R. Dessapt and P. Mialane, *Inorg. Chem.*, 2012, **51**, 2291.
 - 6 K. Hakouk, O. Oms, A. Dolbecq, H. E. Moll, J. Marrot, M. Evain, F. Molton, C. Duboc, P. Deniard, S. Jobic, P. Mialane and R. Dessapt, *Inorg. Chem.*, 2013, **52**, 555.
 - 7 J.-D. Compain, P. Deniard, R. Dessapt, A. Dolbecq, O. Oms, F. Secheresse, J. Marrot and P. Mialane, *Chem. Commun.*, 2010, **46**, 7733.
-